Pharm Res (2012) 29:1977–1989
DOI 10.1007/s11095-012-0725-5

RESEARCH PAPER

Stability Influences the Biodistribution, Toxicity, and Anti-tumor Activity of Doxorubicin Encapsulated in PEG-PE Micelles in Mice

Xiuli Wei • Yiguang Wang • Wenfeng Zeng • Feng Huang • Lei Qin • Chunling Zhang • Wei Liang

Received: 11 October 2011 / Accepted: 27 February 2012 / Published online: 17 March 2012

ABSTRACT

Purpose To investigate the influences of stability of doxorubicin (DOX) retained in PEG-PE/HSPC micelles on its biodistribution, toxicity and anti-tumor activity in mice.

Methods We incorporated HSPC into PEG-PE micelles at various molar ratios by a self-assembly procedure. Micelles were characterized by dynamic light scattering, transmission electron microscope, atomic force microscopy. Agarose gel electrophoresis assay was used to detect stable retention of DOX in micellar preparations. Biodistribution, toxicity and anti-tumor activity of doxorubicin encapsulated in PEG-PE/HSPC micelles in mice were investigated.

Results HSPC incorporation not only changed the size and shape of PEG-PE micelles, but also decreased the ability of DOX stable retained in PEG-PE micelles, resulting in a great discrepancy in biodistribution, toxicity and anti-tumor activity among micellar DOX preparations. DOX encapsulated in PEG-PE micelles (M_1-DOX), with narrower size distribution and greater stability, demonstrated better cytotoxicity *in vitro* and low systemic toxicity with superior anti-tumor metastasis activity *in vivo*.

Conclusions Encapsulation of DOX into PEG-PE micelles showed the best therapeutic activity and lowest systemic toxicity compared to other HSPC-incorporated PEG-PE micellar preparations. Stable retention of drugs within micelles is important and is determined by compatibility between drugs and polymer blocks.

KEY WORDS anti-tumor metastasis · biodistribution · PEG-PE/HSPC micelles · stability · toxicity

INTRODUCTION

Nanoparticle is an emerging nanomedicine platform for cancer therapeutic application due to their small size (10–100 nm) and surface properties (1,2). It has been reported that nanoparticle therapeutics can enhance anticancer efficacy, while reduce the side-effects, owing to properties including preferential accumulation in tumor tissue as a result of enhanced permeation and retention (EPR) effect (3) and active intracellular uptake (4). Nanosized self-assembled constructs, such as micelles, have shown many advantages as potential drug delivery systems (5,6). These spherical carriers are formed from the self-assembly of amphiphilic molecules in water. The entrapment of poorly soluble drugs into the hydrophobic core of micelles has been shown to improve the bioavailability and pharmacokinetics of the drugs, as well as provide protection from destruction *in vivo* (7).

Polyethylene glycol-phosphatidylethanolamine (PEG-PE) conjugate, a block copolymer, has been widely used in stealth liposome formulation. It has been reported that micelles comprised of PEG-PE can load with a variety of poorly soluble drugs such as paclitaxel and tamosifen (8), and are capable of delivering their load into low cutoff size tumor in mice with higher efficiency than even PEG-modified liposomes (9). We have demonstrated the nanoassemblies of PEG-PE and DOX increasing cytotoxicity *in vitro* and enhancing anti-tumor activity *in vivo* with low systemic toxicity (10). Recently, we have used a one-step self-assembly procedure to load water-soluble amphiphilic drugs, such as DOX hydrochloride, epirubicin hydrochloride, vinorelbine tartrate and vincristine sulfate, into PEG-PE micelles in aqueous medium. DOX- and vinorelbine-loaded PEG-PE micelles had a very high drug-loading efficiency (> 99 %) (11).

Xiuli Wei and Yiguang Wang contributed equally to this work.

X. Wei · Y. Wang · W. Zeng · F. Huang · L. Qin · C. Zhang · W. Liang
Protein & Peptide Pharmaceutical Laboratory
National Laboratory of Biomacromolecules, Institute of Biophysics
Chinese Academy of Sciences, Beijing 100101, China

C. Zhang (✉) · W. Liang (✉)
National Laboratory of Biomacromolecules, Institute of Biophysics
Chinese Academy of Sciences, 15 Datun Road
Beijing 100101, China
e-mail: zhangcl@moon.ibp.ac.cn
e-mail: weixx@sun5.ibp.ac.cn

Polymeric micelles, as a drug delivery system, meet a significant challenge that is their stability after administration *in vivo*. This is due to micelle stability is a function of both thermodynamic and kinetic parameters. When the concentration of polymers below the critical micelle concentration (CMC), premature micelle should disassemble rapidly and release its payloads quickly (12). To overcome this drawback, two strategies are often used to develop these micelles are able to stably retain the drug for a prolonged time in the circulation before micelles arriving their target for releasing their payloads. One is covalently conjugated drug with copolymer through a pH-sensitive linker (13). Another one is the crosslinked micelles that formed from these polymers with the functionalized groups (14). We have shown that encapsulation of DOX into PEG-PE micelles has a tightly packed structure compared to the PEG-PE micelles without DOX, which allows a longer circulation in plasma and a controlled drug release responded to pH change (10). This is possibly due to the amphiphilic nature of the two molecules as well as their specific structures. In order to distinguish the molecular fitting, instead of the drug molecule wrapping in the PEG-PE micelles encapsulating DOX, we incorporated HSPC into PEG-PE micelles at various molar ratios and used a self-assembly procedure to load DOX into PEG-PE based micelles. HSPC has a higher gel transition temperature (~55 °C) than other PCs, and is one component approved by FDA for liposomal doxorubicin (Doxil). We expect that the incorporated HSPC could have a influence on the interaction between DOX and PEG-PE copolymer, thus, in turn alters the release profile of DOX from the micelles *in vitro* and changes the pharmacokinetics of DOX *in vivo*, resulting in the differences in toxicity and anti-tumor activity. In this study, we investigate how DOX stably retained in micelles influences its biodistribution, toxicity and anti-tumor activity in mice.

MATERIALS AND METHODS

Materials

Distearoyl-*sn*-glycero-3-phosphoethanolamine-*n*-[methoxy (polyethylene glycol) -2000] (PEG-PE) was obtained from Avanti Polar Lipids, Inc. (Alabaster, AL). Hydrogenated phosphatidylcholine (HSPC) was purchased from LIPOID GmbH (Ludwigshafen, Germany). DOX hydrochloride was kindly provided by HaiZheng Pharmaceutical Co. Ltd (Taizhou, Zhejiang, China). Water used throughout was distilled and deionized in a Milli-Q water purification system (Millipore, Bedford, U.K.) All other reagents used were of analytical grade.

Cell Line

MDA-MB-231 human breast adenocarcinoma cells (ATCC No.HTB-26) and 4T1 mouse mammary tumor cells (ATCC No.CRL-2539) were purchased from American Type Culture Collection (ATCC; Manassas, VA). MDA-MB-231 cells and 4T1 cells were cultured in L15 and RPMI 1640 medium supplemented with 10 % heat-inactivated fetal bovine serum (FBS), respectively. Cell culture medium and FBS were from Invitrogen (Carlsbad, CA). Culture flasks and dishes were from Corning (Corning, New York, NY).

Animals

BALB/c female mice (6–8 weeks old) were provided by Institute of Materia Medica, Chinese Academy of Medical Sciences. Food and water were provided *ad libitum*. All animal procedures were performed following the protocol approved by the Institutional Animal Care and Use Committee at the Institute of Biophysics, Chinese Academy of Sciences.

Preparation of DOX Loaded in Micelles

DOX-loaded micelles were prepared by a one-step self-assembly method. Briefly, DOX hydrochloride was dissolved and PEG-PE was suspended in Milli-Q water. PEG-PE/HSPC mixed suspension was prepared by co-dissolving PEG-PE and HSPC in chloroform, and then slowly evaporated by rotary evaporator. The lipid film was hydrated with Milli-Q water. Equal volume of drug solution and PEG-PE/HSPC suspension was mixed and incubated for 30 min at 60 °C. Followed by addition of mannitol (5 %, w/v) to the mixture, the micelle preparations were filtered using 0.22 μm polyethersulfone syringe membrane. The final concentration of doxorubicin in the filtered micelles was 2 mg/ml as determined by high-performance liquid chromatography (HPLC), and then were lyophilized and stored at 4 °C for further investigation. The degraded products of doxorubicin incorporated in micelles were detected using HPLC after defined periods of storage. Based on the molar ratios of PEG-PE/HSPC/DOX, the three micellar preparations were named as M_1-DOX (PEG-PE:HSPC:DOX=1:0:1), M_2-DOX (PEG-PE:HSPC:DOX=1:0.5:1) and M_3-DOX (PEG-PE:HSPC:DOX=1:1:1), respectively.

Characterization of Three Micellar Preparations

Particle size distribution and zeta potential of doxorubicin-loaded micelles were determined by dynamic light scattering (DLS) analysis using Nano Particle Analyzer (Malvern Instrument Ltd, Malvern, UK). The morphology of three micellar preparations was observed via transmission electron microscope (TEM, FEI Tecnai G-20, Netherlands) and atomic force microscopy (AFM, Multimode SPM, Nanoscope IIIA, USA). Integrity and stability of micellar DOX preparations in 5 % (v/v) serum were examined through 1 % agarose gel electrophoresis.

The samples (containing 1 mg/ml of DOX) were incubated with or without 5 % serum at 37 °C for 30 min before electrophoresis. Drug encapsulation efficiency of DOX was determined by ultrafiltration. Briefly, 500 μL of micellar doxorubixin formulations or free-doxorubicin (2 mg/ml) were added in amicon ultra centrifugal filter devices (MWCO 30,000, Millipore), and then centrifuged at 12000×g for 10 min at 4 °C. The concentrations of free drugs in filtrate were quantified by reverse-phase HPLC with a C18 column (Hypersil, ODS2, 5 μm, 4.6×150 mm, National Chromatography R&A Center, Dalian, China). The detection wavelength was 254 nm, and the mobile phase was composed of sodium dodecylsulfate (SDS) solution (1.44 g of SDS and 0.68 mL of phosphoric acid were co-dissolved in 500 ml of Milli-Q water)-acetonitrile-methanol (500:500:60, v/v/v). The *in vitro* release profile of DOX from three micellar preparations was monitored using equilibrium dialysis method as described previously (11).

Cellular Uptake and Cytotoxicity of DOX from Three Micellar Preparations

To measure the internalization of DOX quantitatively, MDA-MB-231 cells were cultured on 6-well plates (10^5 cells/well) for 24 h to achieve approximately 80 % confluence. Each of three micellar DOX preparations or F-DOX (DOX concentration, 1.7 μM) was then added to designated wells. After incubation for 12 h, the cells were washed and collected in ice-cold phosphate-buffer saline for measurement of DOX fluorescence. The fluorescence from individual cells was detected with a flow cytometer (FACS Calibur, BD, San Jose, CA) as described previously (10). For detection of doxorubicin-derived fluorescence, excitation was with the 488 nm line of an argon laser and emission fluorescence between 564 and 606 nm was measured. For all experiments in which the intracellular doxorubicin was quantified using flow cytometer at least 10000 cells were measured from each sample.

The Cytotoxicity of F-DOX and three micellar DOX preparations against MDA-MB-231 cells was evaluated by MTT assay. Cells were seeded in 96-well plates (5×10^3 cells/well) and allowed to attach to the plate surface for 24 h, and then exposed to a series of concentrations of F-DOX or three micellar DOX preparations for 48 h, and the viability of cells was measured. The mean percentage of cell survival relative to that of untreated cells and 95 % confidence intervals (CIs) were estimated from data in three individual experiments. The concentration of DOX at which 50 % cell killed was calculated by curve fitting using SPSS software.

Biodistribution Study

Subcutaneously, 0.1 ml of cell suspension containing 1.5×10^5 4T1 cells was injected into a mammary gland in the lower right quadrant of the abdomen of BALB/c female mice. When the diameter of primary tumor reaches to about 5–10 mm, 144 mice were randomly divided into the following four treatment groups (n=36 mice per group): F-DOX, M_1-DOX, M_2-DOX and M_3-DOX. Each treatment group was given by tail vein injection at a dose of 10 mg/kg DOX. Blood samples were collected at 1, 3, 6, 12 and 24 h. Heart, liver, spleen, lung, kidney and tumors were collected at 3, 12 and 24 h, and then washed, weighted and homogenized in 5 volumes of acidic ethanol (0.3 M HCl:EtOH, 3:7, v/v) with tissue homogenizer (IKA®, T10 basic Homogenizer Workcenter, Sigma). The amount of DOX in plasma and tissue homogenate was detected with a fluorometer. For pharmacokinetics, DOX concentration is expressed as microgram per milliliter of blood plasma. For biodistribution, DOX concentration is expressed as microgram per gram of tissue. Area under the plasma time-curve from 0 to 24 h (AUC_{0-24}) was calculated using the trapezoidal rule.

Toxicity Assay

The acute toxicity was generally defined as the adverse effects occurring within a short time after administration of a single dose or multiple doses of a substance, continuously observed for 7–14 days. The acute toxicity of F-DOX, M_1-DOX, M_2-DOX and M_3-DOX were evaluated by administering intravenously via the tail vein to BALB/c female mice, and 0.9 % sodium chloride was serviced as control.

420 BALB/c femal mice were randomized into one of the following five groups: control, F-DOX and three micellar preparations. The each of F-DOX and three micellar DOX preparations groups were further divided into five sub-groups that correspond to the dose levels of 9.6, 12.7, 16.9, 22.5 and 30 mg/kg with a fixed-dose increment (1:1.33) between consecutive doses (n=20 mice per group). Animals were monitored for possible signs of toxicity including the general conditions and body weight, and the survival situation were monitored daily for two weeks. On day 7, 6 mice from 9.6 and 16.9 mg/kg treatment groups were sacrificed by cervical vertebra dislocation, blood samples were collected for blood routine analysis (Sysmex kx21 autoanalyzer, Japan) and blood chemistry analysis (Hitachi 7600p autoanalyzer, Japan). Heart, liver, spleen, lung and kidney were preserved in 10 % buffered formaldehyde. Once the tissue processed and embedded in paraffin, 5 μm sections were cut and stained with routine Haematoxylin and Eosin staining for histopathological examination.

To further determine the toxicity of F-DOX and three micellar DOX preparations to major organs from Balb/C mice, an *in situ* cell death detection kit (Fluordescein, Roche diagnostics, USA) according to the manufacturer's instructions was used. Mice were randomly divided into the following five treatment groups: control, F-DOX, M_1-DOX, M_2-DOX and M_3-DOX. The drugs were given by bolus tail

vein injection at a dose of 16.9 mg/kg. There were 5 animals for each treatment. After 6 h, major organs including liver, heart, spleen, lung and kidney were collected and fixed in 4 % paraformaldehyde in PBS for paraffin embedding. The sections were used for detection of apoptotic cells by TUNEL method.

In Vivo Therapeutic Study

BALB/c mice bearing 4T1 tumors were subjected to examine *in vivo* anti-tumor metastasis activity. When the primary tumor volume reaches to about 100–200 mm^3, Mice were randomly assigned to one of the following five treatment groups (n=10 mice per group): control, F-DOX and three micellar DOX preparations (10 mg/kg each). Mice were treated through tail vein injection on day 7 and day 14. Mice were sacrificed by cervical vertebra dislocation on day 28, and their lungs were immediately harvested and weighted. Pulmonary metastasis was also evaluated by counting tumor nodules in the each lung.

Statistical Analysis

Data were expressed as means ± SD unless noted otherwise. Statistical analysis was performed by one-way ANOVA and followed by Bonferroni's post-test using Stata software (version 7.0). Survival was assessed with the Kaplan-Meier method, and Log-rank (Mantel-Cox) test was used to compare the survival curve. P values less than 0.05 were considered to be statistically significant.

RESULTS

Preparation and Characterization of PEG-PE-Based Micelles Encapsulating DOX

We incorporated HSPC into PEG-PE micelles up to a molar ratio of HSPC to PEG-PE of 1 to 1. The mean diameter of M_1-DOX made from PEG-PE copolymer was 14.5 ± 1.2 nm, consistent with our previous works (10,11). The increased sizes were observed in the micelles incorporated 33 % (M_2-DOX) and 50 % (M_3-DOX) of HSPC, with diameter of 22.4 ± 0.9 nm, and 34.2 ± 1.3 nm, respectively. Meanwhile, the morphology of micelles observed by TEM showed that HSPC incorporation led to change the size and shape of PEG-PE micelles encapsulating DOX, as shown in Fig. 1a–c. The morphology of M_1-DOX was intact and well-defined spherical style with narrow size distribution, while the incorporated HSPC reached to 33 % or 50 % mole, size distribution became broad, and the morphology of micelles were altered from spherical to ellipsoidal or the rod-like, especially for M_3-DOX. The phenomenon observed by TEM was further confirmed by AFM (Fig. 1d–f). Rod or worm-like micelles formed from the increasing ratio of phospholipid in PEGylated phospholipid have been demonstrated by the works of Hristoval *et al.* (15) and Ashok *et al.* (16,17), which are in agreement with our observations.

To determine the effect of HSPC incorporation on the encapsulation and release of DOX, we examined the encapsulation efficiency and release profile of DOX in these micelles. HSPC incorporation did not change the loading efficiency (99.9 % for three micellar preparations) and the release profile of DOX from the micelles using dialysis method (Fig. 1g). DOX was slowly released from three micellar preparations without initial burst release. Less than 50 % DOX was released from the micelles up to 24 h, and the percent of released DOX was 41.9 %, 38.7 % and 39.1 % for M_1-DOX, M_2-DOX and M_3-DOX, respectively. After 24 h, the remains of DOX in dialysis bag were 48.6 %, 48.4 % and 51.6 % for M_1-DOX, M_2-DOX and M_3-DOX, respectively. In contrast, 100 % free DOX was released from dialysis bag within 3 h (data not shown). These data indicate that HSPC incorporation has no obvious effect on the release profile of DOX from three preparations *in vitro*.

Our previous work has revealed that electrostatic interaction between PEG-PE and DOX play a critical role in stable drug encapsulation in the micelle. However, HSPC incorporation did not influence the encapsulation and release of micelle-loading DOX. To test the effect of HSPC incorporation on the stability of DOX retained in PEG-PE micelles, the agarose gel electrophoresis method was used. The same amount of DOX in each preparation was loaded in the wells, F-DOX as a control. As shown in Fig. 1h, free- and released-DOX was moved to the negative electrode due to DOX molecule with a positive charge. However, DOX encapsulated in micelles was moved to positive electrode because their zeta potential was negative, and the value of M_1-DOX, M_2-DOX and M_3-DOX were −35.3, −37.1 and −36.3 mV, respectively. We calculated the released DOX from all three micellar preparations using Bio-capt software (Automatic gel image analyzing system, Infinity 3026, Vilber, French). In the absence of serum, M_1-DOX showed the least released DOX (12.1 %), M_3-DOX showed the most released DOX (28.6 %), and the drug release of M_2-DOX was 22.4 %. When all samples were incubated with 5 % serum for 30 min, the result showed that more than 70 % DOX was released from M_3-DOX while only 13.1 % DOX was released from M_1-DOX. For M_2-DOX, the released DOX in the presence of serum (43.6 %) was two times than in the absence of serum. Taken together, these results indicated that DOX can stably retain in the PEG-PE micelles and is able to resist to serum induced destruction, while HSPC incorporation reduced the interaction of DOX

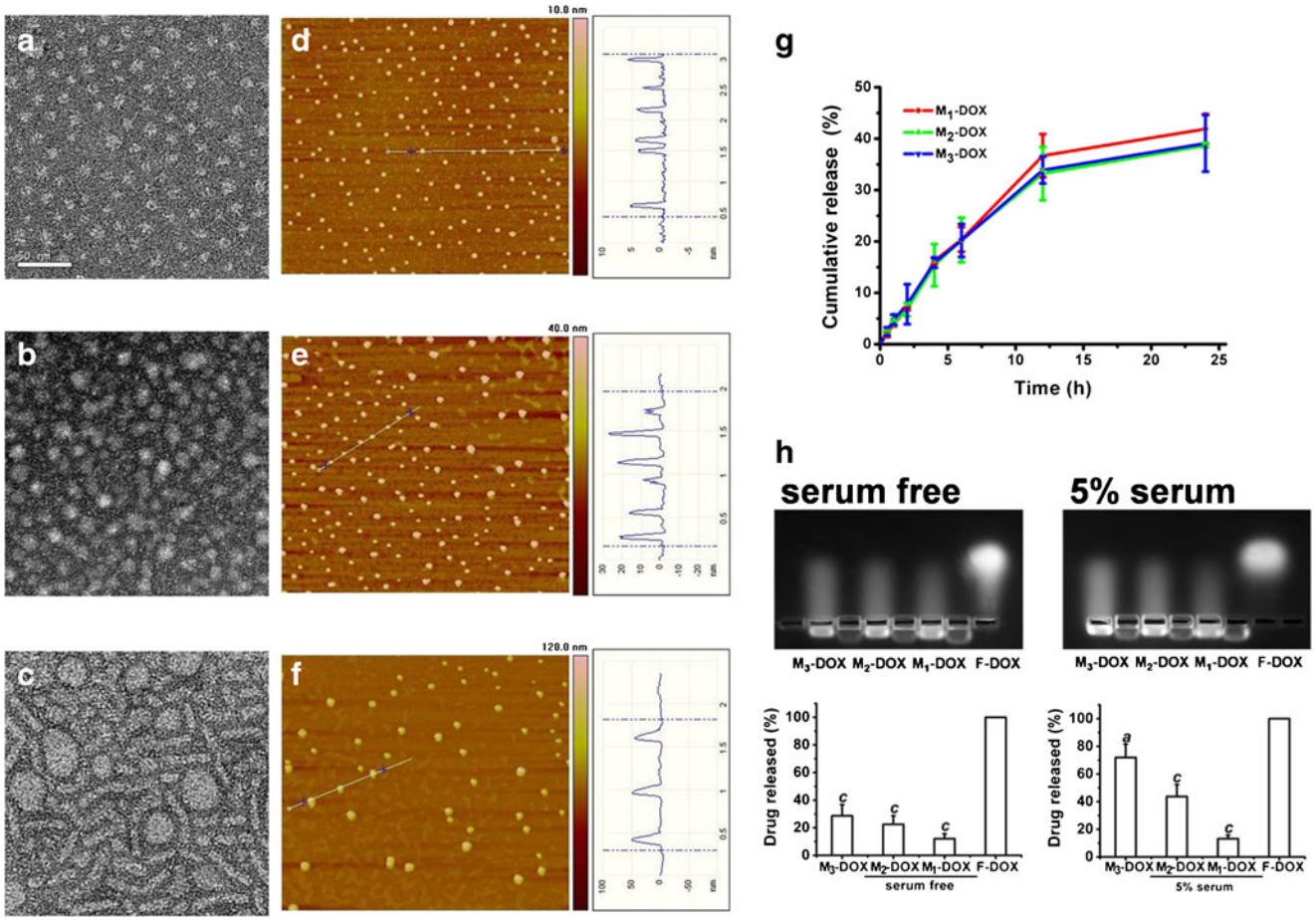

Fig. 1 Characterization of three micellar DOX preparations. TEM (**a**, M_1-DOX, **b**, M_2-DOX, **c**, M_3-DOX, Scale bar is 50 nm) and AFM (**d**, M_1-DOX, **e**, M_2-DOX, **f**, M_3-DOX, Scale bar is 5 μm) images of three micellar DOX preparations. (**g**) *In vitro* release profiles of three micellar preparations in pH 7.4 PBS using dialysis method. (**h**) Gel electrophoresis analysis of three micellar DOX preparations. The released DOX from micelles was measured by semiquantitative analysis. Each point represents the mean ± SD (n=3) from individual experiments. ***a***, $P<0.05$, ***c***, $P<0.001$ *versus* F-DOX.

with PEG-PE copolymer, thus led to a decreased stability of drug load in PEG-PE micelles and a lowered resistance to serum.

In Vitro Cytotoxicity of DOX Encapsulated in Micelles

Firstly, we performed the cellular uptake experiment in MDA-MB-231 cells. Cells were treated with F-DOX or each micellar preparation containing DOX at 1.7 μM for 12 h, and then the cells were collected for measurement of DOX-derived fluorescence intensity by flow cytometry. As shown in Fig. 2a, DOX encapsulated in micelles was taken up by cells much more than its free form, 1.82, 2.01 and 1.83 times more than F-DOX for M_1-DOX, M_2-DOX and M_3-DOX, respectively. The intracellular DOX fluorescent intensity of M_1-DOX (128.25 ± 2.78), M_2-DOX (142.04 ± 0.11) and M_3-DOX (129.41 ± 2.08) had no significant difference. Next, cytotoxicity induced by DOX to MDA-MB-231 cells was determined by MTT assay. The IC_{50} Values of F-DOX, M_1-DOX, M_2-DOX and M_3-DOX were 596.4 ± 125.9 nM, 378.4 ± 85.3 nM, 321.3 ± 86.3 nM and 299.6 ± 60.2 nM, respectively (Fig. 2b). This data indicated that the concentration of DOX in three micellar preparations that caused 50 % killing was much lower than that of F-DOX. For three micellar preparations, the value of IC_{50} slightly decreased with the increased HSPC ratios, but no significant difference. In general, encapsulation of DOX in PEG-PE micelles plays an important role in the enhancement of its cytotoxic activity while HSPC incorporation has a slight influence.

Biodistribution of DOX Encapsulated in Micelles

Many studies have demonstrated that drugs encapsulated in nanoparticles with different stability displays diverse behaviors *in vivo* (18,19). In order to determine PEG-PE-based micelles with different drug retention abilities have an influence on their load biodistribution, the PEG-PE-based micelles prepared by HSPC incorporation showed different drug retention abilities. We then determined the

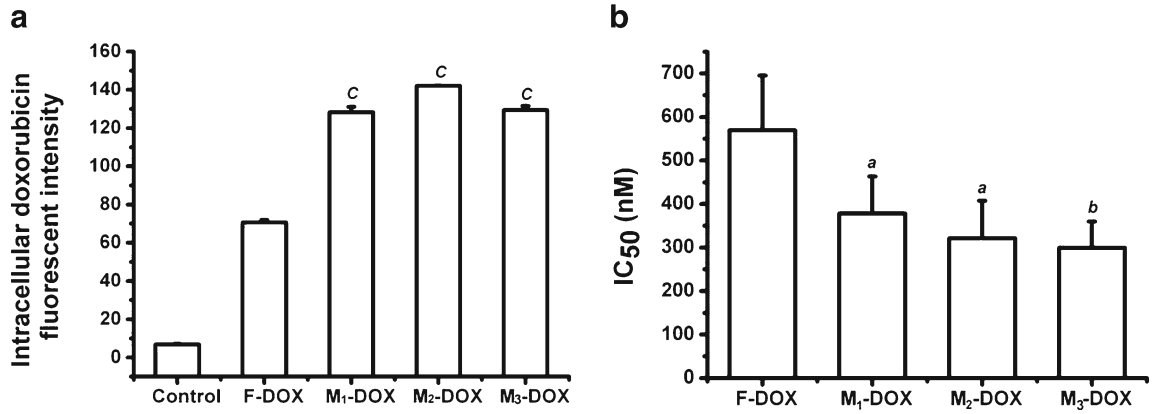

Fig. 2 *In vitro* cellular uptake and cytotoxicity of three micellar DOX preparations and F-DOX aganist MDA-MB-231 cells. (**a**) Intracellular fluorescence intensity was measured by flow cytometry after 12 h treatment with each DOX preparation, (**b**) IC_{50} of three micellar DOX preparations or F-DOX. Each point represents the mean ± SD (n=3) from three independent experiments. (**a**) $P < 0.05$, (**b**) $P < 0.01$, (**c**) $P < 0.001$ *versus* F-DOX.

pharmacokinetics and biodistribution of DOX encapsulated in these micelles As shown in Fig. 3a, at 1 h post-injection, the drug concentration of M_1-DOX, M_2-DOX and M_3-DOX in plasma was 1.34±0.07 μg/ml, 1.24±0.09 μg/ml and 1.11± 0.07 μg/ml, respectively, and approximately 1.74, 1.61 and 1.44 times more than F-DOX. Within 12 h, three micellar DOX preparations showed higher serum drug concentrations than free drug, and M_1-DOX provided the highest peak

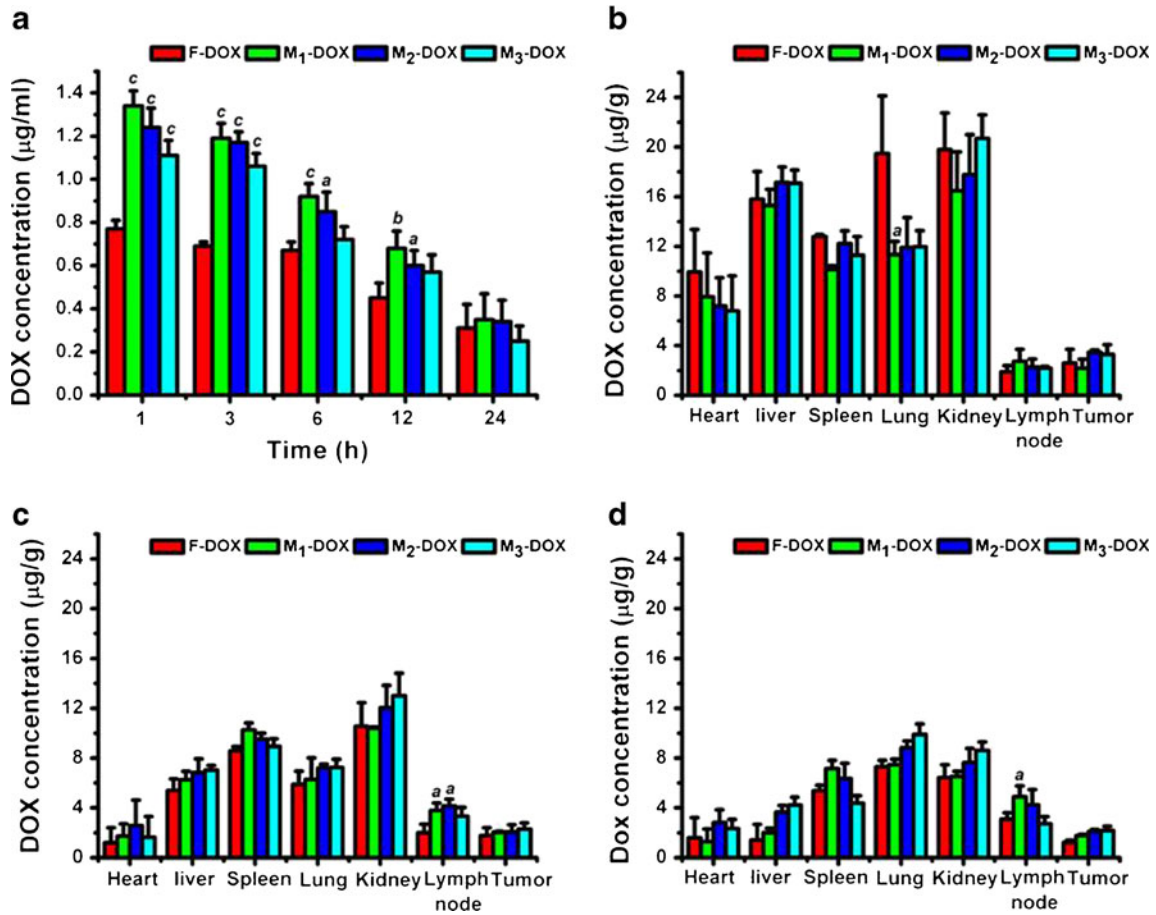

Fig. 3 *In vivo* biodistribution and accumulation of three micellar DOX preparations in 4T1-bearing BALB/c mice subcutaneous model. Mean DOX concentrations in serum (**a**) and major organs at 3 h (**a**), 12 h (**c**) and 24 h (**d**) from mice treated with F-DOX or three micellar DOX preparations. Data represent mean ± SD (n=6) from individual experiments points. (**a**) $P < 0.05$, (**b**) $P < 0.01$, (**c**) $P < 0.001$ *versus* F-DOX.

concentration (C_{max}) values. M_3-DOX displayed the lowest serum drug concentration among three micellar preparations of DOX. AUC_{0-24} of F-DOX, M_1-DOX, M_2-DOX and M_3-DOX was 11.42, 16.71, 15.43 and 13.73 μg·h/L, respectively. M_3-DOX, the formulation with the worst stability in the presence of serum, presented minimum AUC_{0-24} in all three micellar DOX preparations, indicating that the stability of micelles play an important role in the blood drug clearance. Drug concentrations of M_1-DOX, M_2-DOX and M_3-DOX in tumor were 1.15 1.16 and 1.29 at 12 h (Fig. 3c), and 1.44, 1.71 and 1.78-fold at 24 h (Fig. 3d), higher than that of free DOX respectively. These results indicate that EPR effect in tumor besides stability plays an important role in the accumulation of nanocarriers of drug. On the other hand, drug concentrations of M_1-DOX, M_2-DOX and M_3-DOX in liver, lung and kidney showed slight size-dependent accumulation of DOX (Fig. 3b–d) throughout our observation times. As shown in Fig. 3b, for F-DOX, drug concentration at 3 h in heart and lung was 9.94±3.42 μg/g, 19.47±4.65 μg/g, respectively, which was higher than that of all micellar DOX preparations, while in kidney was 19.8±3.42 μg/g, higher than that of M_1-DOX and M_2-DOX, and slight lower than that of M_3-DOX, indicating the potential toxicity of F-DOX to these organs. Interestingly, M_1-DOX showed a lymph node tropism, the increased drug concentration in lymph node was observed throughout our experiment times, was 2.72±0.98 μg/g, 3.79±0.59 μg/g and 4.88±0.89 μg/g at 3, 12, and 24 h after injection, respectively. This data indicated that M_1-DOX may have a potential to treat tumor metastasis through lymphatic pathway.

Acute Toxicity of DOX Encapsulated in Micelles

We tested survival and toxicity in mice received a single dose. Mice received F-DOX or each micellar DOX preparation with different dosages showed adynamia, tremor, piloerection, diarrhoea and loss of weight. These adverse effects were dose-dependent for all preparations of DOX. The adverse effects caused by micellar DOX preparations were less than F-DOX. Diarrhoea was observed on day 2 at the dose of 30 mg/kg in mice treated with F-DOX and three micellar DOX preparations. The dead mouse was associated with continuous loss of weight, adynamia, tremor and piloerection. Peaks of death after administered 30 mg/kg dose of F-DOX and three micellar DOX preparations were observed on days 3–5 and 5–7, respectively. All mice treated with the maximal dose of F-DOX and three micellar DOX preparations were dead within 7 days. When the dose decreased to 22.5 mg/kg, mortality of mice between F-DOX and micellar DOX preparations was markedly difference. At day 7, mortality was 100 %, 30 %, 60 % and 70 % for F-DOX, M_1-DOX, M_2-DOX and M_3-DOX, respectively. Mice treated with M_1-DOX showed increased life span compared to M_2-DOX, M_3-DOX or F-DOX (Fig. 4a). The survival curve of M_1-DOX ($P<0.01$) was significant difference from F-DOX. When the dose further decreased to 16.9 mg/kg, the survival curves of mice were also markedly different ($P<0.01$ *versus* F-DOX). Mortality of F-DOX, M_1-DOX, M_2-DOX and M_3-DOX was 80 %, 0 %, 40 % and 60 % respectively (Fig. 4b). The results indicate that DOX encapsulated in PEG-PE-based micelles can reduce its systemic toxicity. The more stability of DOX in micelles is related to the less toxicity.

On day 7, blood samples were taken from the following groups of mice administered with 9.6 mg/kg (low dose) and 16.9 mg/kg (high dose), biochemical parameters including alanine amiotransferase (ALT), aspartate amiotransferase (AST), total protein (TP), albumin (ALB), creatine kinase isoenzyme (CK-MB), lactate dehydrogenase (LDH), urea nitrogen (BUN) and creatine kinase were measured in the serum as markers of organic injury. Regarding liver function, compared to normal control, elevations in ALT were always

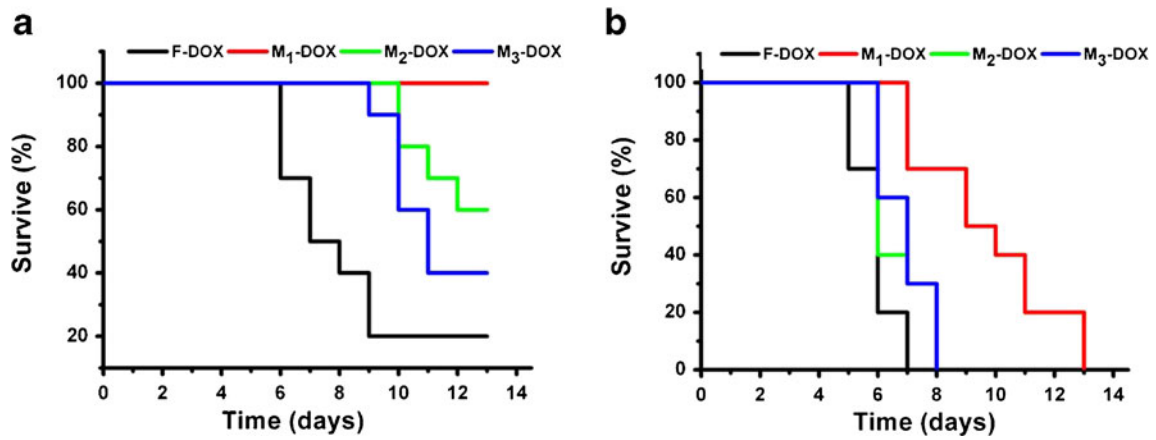

Fig. 4 Kaplan-Meier graphs showing survival of BALB/c mice treated with a single dose of 22.5 mg/kg (**a**) and 16.9 mg/kg (**b**) of three micellar DOX preparations or F-DOX.

detected in each group of mice administered DOX, and were dose-dependent. At high dose of 16.9 mg/kg, the ALT concentrations of mice received F-DOX, M_1-DOX, M_2-DOX and M_3-DOX were 48.38±9.98 IU/L, 42.89±8.27 IU/L, 39.00±7.15 IU/L and 44.89±3.92 IU/L, respectively. Although F-DOX induced much more elevated ALT concentration, the difference between F-DOX and micellar DOX preparations had no statistical significance. At low dose of 9.6 mg/kg, the elevated concentration of ALT induced by micellar DOX preparations was almost similar (Fig. 5a). Elevations in AST were not observed in each group of mice administered with DOX (data not shown). At low dose of 9.6 mg/kg, F-DOX and micellar DOX preparations did not have an influence on the concentration of TP and ALB. However, increasing dose to 16.9 mg/kg, F-DOX and three micellar DOX preparations resulted in the remarkable drop compared with normal control. The TP and ALB concentration of mice received F-DOX, M_1-DOX, M_2-DOX and M_3-DOX were 42.53±3.10 and 19.94±2.26 g/dL, 47.78±3.92 and 26.34±4.77 g/dL, 46.42±7.15 and 26.34±4.77 g/dL, and 48.09±3.58 and 27.34±4.42 g/dL, respectively. F-DOX caused the decrease of ALB and TP was much more than three micellar DOX preparations. There was no difference between three micellar DOX preparations (Fig. 5b and c). A profound reduction in peripheral leukocyte count, characterized by marked reductions in white blood cell (WBC) and lymphocytes (LYM) was observed on day 7 after F-DOX administration in the dose-dependent manner, the number of WBC and LYM were $(6.23\pm0.94)\times10^9$ and $(4.80\pm0.83)\times10^9$/L at the dose of 9.6, and $(4.20\pm0.72)\times10^9$ and $(3.10\pm0.68)\times10^9$/L at the dose of 16.9 mg/kg. At low dose of 9.6 mg/kg, the reduction in WBC and LYM was not observed after three micellar DOX preparations administration. The number of WBC treated with M_1-DOX, M_2-DOX or M_3-DOX at high dose of 16.9 mg/kg was $(5.80\pm0.81)\times10^9$/L, $(5.44\pm0.95)\times10^9$/L and $(5.50\pm0.70)\times10^9$/L, respectively. Compare with control, micellar DOX preparations administration resulted in a marked reduction in the number of WBC, while less than that of F-DOX administration (Fig.6a). M_2-DOX and M_3-DOX at high dose of 16.9 mg/kg also resulted in a marked reduction in LYM [M_2-DOX: $(4.16\pm0.52)\times10^9$/L; M_3-DOX: $(4.67\pm0.24)\times10^9$/L], but M_1-DOX [$(6.17\pm0.89)\times10^9$/L] did not (Fig. 6b). Platelet counts were normal after F-DOX and micellar DOX administration (data not shown).

Histopathology and TUNEL assay of major organs from mice that treated with 16.9 mg/kg of F-DOX or three micellar DOX preparations were performed. Compared to control, there were significant histologic changes in kidney in all treated groups, including homogeneous red exudates in the cavity of glomerular capsule, swelling of renal tubular epithelial cell, and erythro-stained protein casts in some lumina of renal tubule. F-DOX treatment showed more serious kidney lesion than that of micellar DOX preparations. M_1-DOX demonstrated mild kidney lesion in all three micellar DOX preparations (Fig. 7a). There were significant differences in the number of apoptotic cells in kidney and liver between F-DOX and micellar DOX preparations, M_1-DOX showed the very slight kidney damage that TUNEL-positive cells was minimum (Fig. 7b). The degree of apoptosis in kidney further confirmed the results of histopathologic observation. The kidney injury induced by DOX is due to its elimination through kidney (20). The numbers of apoptotic cells in the liver were significant difference between F-DOX and micellar DOX preparations (6 h), while obviously pathological changes were not observed (7 d), this discrepancy may be due to the strong recovery function of liver. Compared to other organs, pulmonary collapse and more apoptotic cells were only observed in the lungs from those mice received F-DOX, which could relate to the high drug concentration in the lungs (Fig. 3b). On the other hand, no significant histopathological change was observed in the lungs from all animals in these groups administrated micellar DOX preparations (Fig. 7a). We did not find any significant histological changes and DNA fragment in heart from all treated mice. In

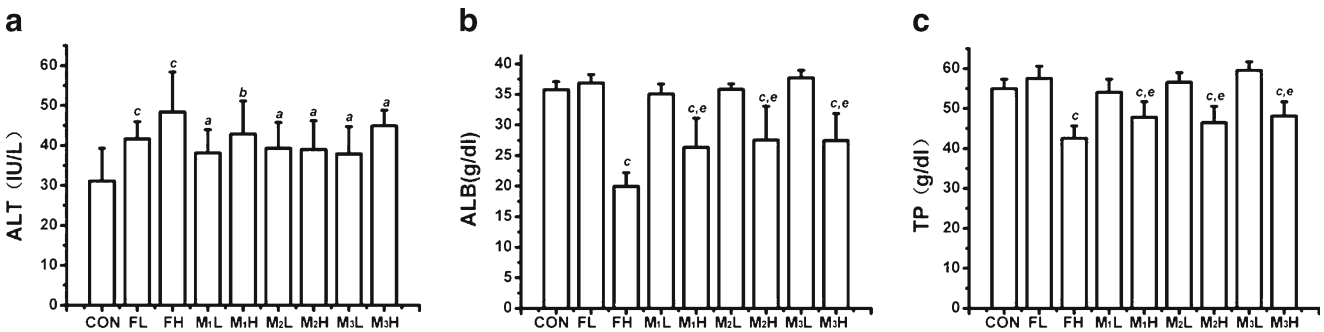

Fig. 5 Serum biochemical parameters (ALT, TP, ALB) of BALB/c mice treated with each preparation at 9.5 and 16.9 mg/kg of DOX. FL, M_1L, M_2L and M_3L are the abbreviation of F-DOX, M_1-DOX, M_2-DOX and M_3-DOX at dose of 9.5 mg/kg, FH, M_1H, M_2H and M_3H are the abbreviation of F-DOX, M_1-DOX, M_2-DOX and M_3-DOX at dose of 16.9 mg/kg, respectively. Data represent mean ± SD (n=6) from individual experiments. (**a**) $P<0.05$, (**b**) $P<0.01$, (**c**) $P<0.001$ *versus* Control, (**e**) $P<0.01$ *versus* F-DOX, respectively.

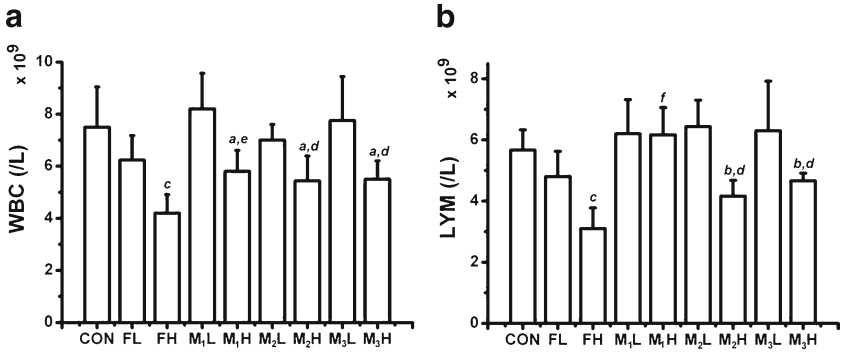

Fig. 6 Blood routine analysis (WBC, LYM) of BALB/c mice treated with each preparation at 9.5 and 16.9 mg/kg of DOX. Data represent mean ± SD ($n=6$) from individual experiments. (**a**) $P<0.05$, (**b**) $P<0.01$, (**c**) $P<0.001$ *versus* Control, (**d**) $P<0.05$, (**e**) $P<0.01$, (**f**) $P<0.001$ *versus* F-DOX, respectively.

general, three micellar DOX preparations, M_1-DOX in particular, showed less toxicity than F-DOX. This may due to the released DOX form M_1-DOX is the least among three micellar DOX preparations.

In Vivo Anti-tumor Metastasis

To address whether PEG-PE-based micelles encapsulating DOX have a superior anti-tumor metastasis to F-DOX, BALB/c mice-bearing 4T1 tumors were treated with 10 mg/kg of F-DOX or each micellar DOX preparation. At day 28, we weighted the lungs weight and counted the number of metastatic nodules in the lungs. Mice treated with M_1-DOX showed a few metastases (Fig. 8b and d), which was 2-fold fewer tumor cell metastases than the mice treated with F-DOX (Fig. 8a and c). However, the mice treated with M_2-DOX or M_3-DOX had an extensive tumor burden in the lungs that was similar to the mice treated with F-DOX (Fig. 8a and d). The inhibitory effect on metastasis of M_1-DOX was reflected in a statistically significant reduction in tumor weight in the lung at day 28 compared with control (Fig. 8c). Treatment with F-DOX, M_2-DOX and M_3-DOX did not cause a statistically significant reduction in the lung tumor burden weight compare with control. The differences among micellar DOX preparations in their anti-tumor metastasis ecffects mainly reflected in the different stability of DOX in these micelles.

DISCUSSION

In this study, we have prepared PEG-PE based three micellar DOX formulations by incorporation of HSPC at various molar ratios with a self-assembly procedure. HSPC incorporation not only changed the size and shape of the micelles formed from PEG-PE copolymers, but also decreased the ability of DOX stable retained in PEG-PE micelles resulting in a great discrepancy in biodistribution, toxicity and anti-tumor activity among micellar DOX preparations.

Chemotherapeutic agents usually caused the does-dependent severe side effects, which most directly related to peak plasma and/or tissue concentration of each drug, such as DOX, most serious being specific cardiotoxicity (21). To reduce exposure of normal tissues to high concentration of chemotherapeutic agents, a successful approach is used to decrease the rate of drug release into blood from carriers, one of them is liposome. Only those liposomes that retain their drug load over several hours to days can obtain a good therapeutic effect and a lower toxicity to body. If liposomes release their drug content at a rate that is faster than the rate of tissue accumulation, then their therapeutic activity could be compromised (19). However, the released drug must reach a minimum cytotoxic concentration, thus bioavailable drug then is able to exert its therapeutic activity. In the current study, administration of M_1-DOX yielded not only the lowest systemic toxicity, but also the best therapeutic activity of the preparations tested, even though M_1-DOX had the slowest rate of DOX release. This suggests that drug is bioavailable at levels above the minimum therapeutic dose.

Using a conventional dialysis method to measure the release of DOX from micelles, we did not discriminate what difference in drug release feature among three micellar DOX preparations. Previous study in our laboratory has demonstrated that there is a strongly electrostatic interaction between DOX and PEG-PE molecules (11). Incorporation of DOTAP, a lipid with positive charge, disrupted this interaction and markedly decreased the encapsulation of DOX into PEG-PE micelles, while HPSC incorporation did not influences the loading efficiency of DOX in micelles, this might be due to the HPSC without positive charge. To test the effect of HPSC incorporation on the interaction between DOX and PEG-PE, the agarose gel electrophoresis method was employed. We found that the increase of the incorporated HSPC proportion induced more drug release from micelles under the electric field, suggesting that the HSPC incorporation decreases the electrostatic interaction of doxorubicin with PEG-PE by increasing the distance between these two molecules.

Animal experiments revealed different behaviors among the tested four DOX preparations: F-DOX, M_1-DOX, M_2-DOX and M_3-DOX (Fig. 3). F-DOX showed the fastest clearance from the blood. At 3 h, F-DOX showed the highest drug accumulation in heart and lung, suggesting its toxicity to

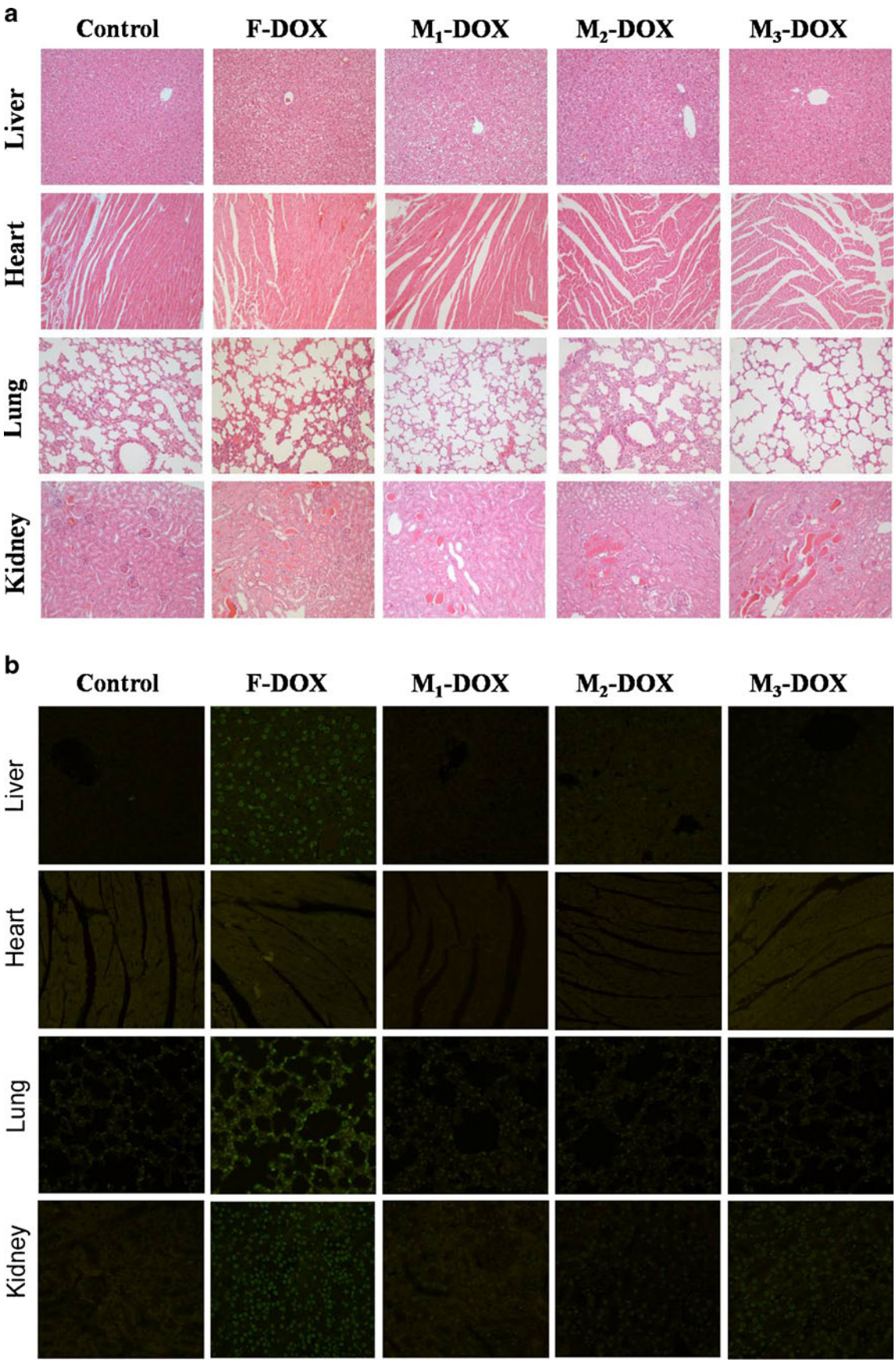
a
Control
F-DOX
M1-DOX
M2-DOX
M3-DOX
Liver
Heart
Lung
Kidney
b
Control
F-DOX
M1-DOX
M2-DOX
M3-DOX
Liver
Heart
Lung
Kidney

◀ **Fig. 7** Histological changes and apoptosis of BALB/c mice treated with a single dose of 16.9 mg/kg of three micellar DOX preparations or F-DOX. Liver, heart, lung and kidney were harvested and subjected to H&E staining (**a**) and TUNEL assay (**b**). × 200 in the original.

these organs are more than M_1-DOX, M_2-DOX and M_3-DOX. This result was similar to liposomal DOX, that showed less signs of toxicity to heart and kidney is due to a lower cumulative dose of DOX in these tissues, compared to administration of free drug (22). DOX from the M_3-DOX with a large size and the lowest drug retention was the fastest cleared from the blood and more accumulated in kidney among three micellar DOX preparations. The distribution of drug in lymph nodes was large different in all DOX preparations. M_1-DOX showed a high accumulation in the lymph nodes compared to other preparations, which could contribute to its good anti-tumor metastasis activity.

We tested the toxicity of DOX *in vitro* and *in vivo*, and found that three micellar preparation of DOX showed more toxicity to MDA-MB-231 cells than F-DOX by improving the cellular drug concentration (Fig. 2), while they had the low toxicity *in vivo* compared to F-DOX (Figs. 4–7). In comparison to F-DOX, M_2-DOX and M_3-DOX, administration of M_1-DOX resulted in the delayed and reduced mortality of mice, and protected lung and kidney injury. Which was due to the slowest release of drug from M_1-DOX and the resistance to the induced destroy by plasma.

In infectious hepatitis and other inflammatory conditions affecting the liver, ALT and AST in serum are typically much higher than their normal levels. These are specific signs of liver damage. There are significant changes for both liver-specific enzymes (ALT and AST) after administration of DOX to animals (23). Our results only observed the elevation of ALT in a dose-dependent manner but not AST for both F-DOX and three micellar DOX preparations treatments. Micellar DOX preparations induced ALT elevation was less than F-DOX. An increase of ALT without significant changes in AST may be typical of liver injury because ALT is a more liver-specific enzyme. In TUNEL test, M_1-DOX induced apoptosis was less then F-DOX and M_2-DOX and M_3-DOX other two micellar preparations. This result further confirmed that F-DOX and micellar DOX preparations with incorporated HSPC led a stronger liver injury due to the exposure of liver to a high drug concentration. Recent study has demonstrated that DOX-induced heart injury is associated with high AST concentration in serum without significant changes in ALT (24).

The elevation of serum concentration of cardiac isoenzymes such as creatine kinase isoenzyme (CK-MB) and lactate dehydrogenase (LDH) is well know quantitative

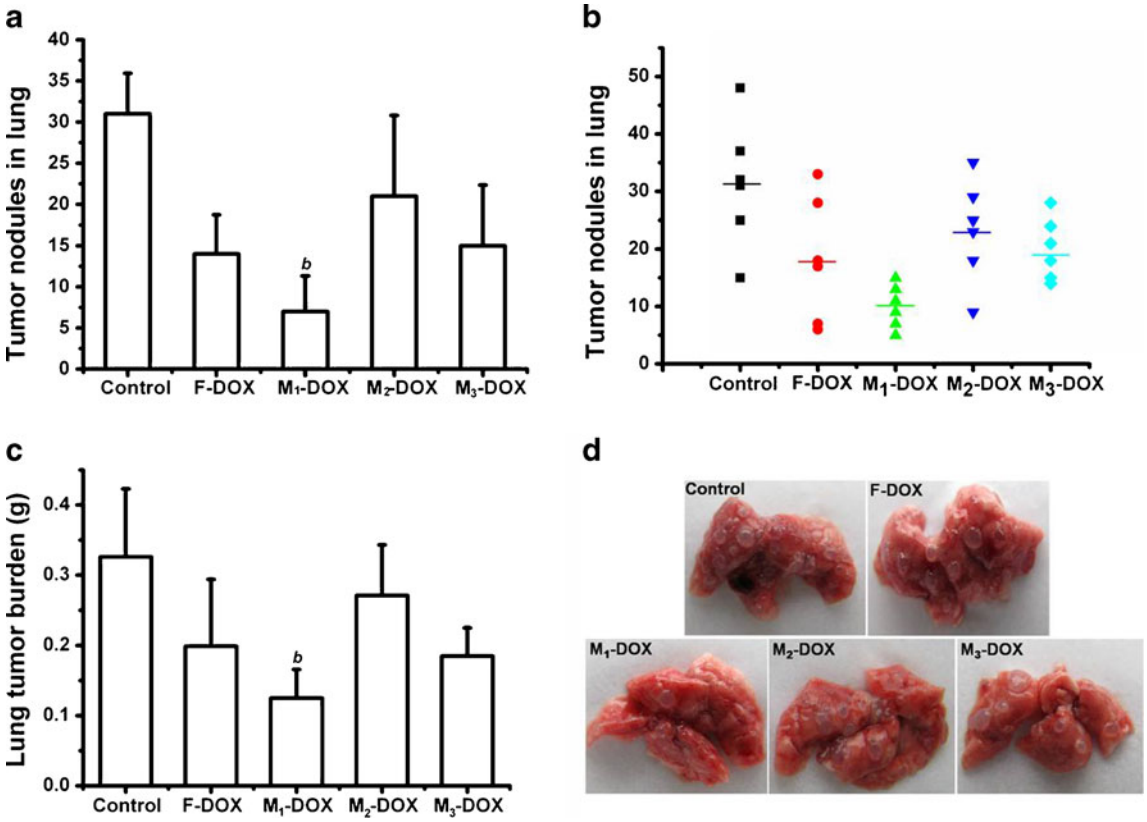

Fig. 8 Anti-tumor metastatic activity of three micellar DOX preparations or F-DOX in 4T1-bearing BALB/c mice subcutaneous model. (**b**) $P < 0.01$ *versus* Control.

index of compromised cell integrity, and is also considered as an indicator of myocardial damage induced by DOX. We examined the serum concentrations of CK-MB and LDH from each group of mice treated with F-DOX or three micellar preparations of DOX. In comparison to normal control mouse, we did not observe a significant change of CK-MB or LDH in serum. Furthermore, we determined the histopathological changes and apoptosis in heart tissue induced by DOX. No histopathological change and obvious apoptosis were observed in the heart from all animals in a single dose of 16.9 mg/kg F-DOX or three micellar DOX preparations (Fig. 7). Taken together with the change of AST, these findings suggest that DOX induces an acute toxicity to other organs such as liver, kidneys and lung rather than heart. The toxicity of DOX to heart is a chronic and lethiferous.

As shown in this study, DOX may have chronic effects on the kidney. Renal function in those mice administrated DOX was fairly well preserved until the terminal of experiments. Both BUN and serum creatinine on day 7 were as the same as the controls, even at high dose of drugs. However, the renal destruction and apoptosis were observed in all animals administrated each DOX preparation. These findings are compatible with previous observations in rats (25,26). The minimal changes in the kidney tissue were seen at week 4, and vacuolation and swelling of epithelial cells were observed at week 8. DOX encapsulated in the micelle significantly alleviated the kidney damage compared to its free form (Fig. 7). In contrast to animals, consistent DOX-induced nephrotoxicity in humans is not evident. Species-related variations in the toxicity of anthracycline have been demonstrated in the kidney and heart (27). Unique long-term toxic effects on kidneys have been observed only in rats and rabbits, while effects on the heart were seen in humans, rabbits, monkeys, and dogs (28). We also observed the toxic effects of DOX on lungs in mice in this study (Fig. 7).

There are two reasons to explain for the observed the reduction of systemic toxicity after administration of M_1-DOX: 1) DOX encapsulated in PEG-PE micelles showed the slowest release of drug and the resistance to the induced destroy by plasma, thus avoids the exposure of the important organs such as heart, liver and kidney to high concentration of free drug. 2) Serum albumin levels do not decrease so much as free DOX due to less toxicity to kidney. This may indirectly have a favorable effect on myocardial function and structure (29).

For the preventing lung metastases, Administration of M_1-DOX demonstrated the least metastatic nodes in lung compared to the other two preparations of DOX. A high level of DOX both in the circulation and in the lymph nodes was found after administration of M_1-DOX, thus may contribute to its enhanced anti metastatic effect.

CONCLUSION

DOX encapsulated in PEG-PE micelles, M_1-DOX, with narrower size distribution and greater stability, demonstrated a high cytotoxicity *in vitro* and a low systemic toxicity with superior anti-tumor metastasis activity *in vivo*, which resulted from the changes of pharmacokinetics and biodistribution of DOX by stably retained in micelles.

ACKNOWLEDGMENTS & DISCLOSURES

This work was supported by grants from State Key Development Plan Project (2007CB935801), the National Nature Sciences Foundation of China (30901869).

Dr Junfeng Hao of the IBP core facilities centre was gratefully thanked for her help for Histopathology and TUNEL assay.

REFERENCES

1. Davis ME, Chen ZG, Shin DM. Nanoparticle therapeutics: an emerging treatment modality for cancer. Nat Rev Drug Discov. 2008;7:771–82.
2. Peer D, Karp JM, Hong S, Farokhzad OC, Margalit R, Langer R. Nanocarriers as an emerging platform for cancer therapy. Nat Nanotechnol. 2007;2:751–60.
3. Maeda H, Wu J, Sawa T, Matsumura Y, Hori K. Tumor vascular permeability and the EPR effect in macromolecular therapeutics: a review. J Contr Release. 2000;65:271–84.
4. Byrne JD, Betancourt T, Brannon-Peppas L. Active targeting schemes for nanoparticle systems in cancer therapeutics. Adv Drug Deliv Rev. 2008;60:1615–26.
5. Sawant RR, Torchilin VP. Polymeric micelles: polyethylene glycol-phosphatidylethanolamine (PEG-PE)-based micelles as an example. Meth Mol Biol. 2010;624:131–49.
6. Nishiyama N, Morimoto Y, Jang WD, Kataoka K. Design and development of dendrimer photosensitizer-incorporated polymeric micelles for enhanced photodynamic therapy. Adv Drug Deliv Rev. 2009;61:327–38.
7. Torchilin VP. Structure and design of polymeric surfactant-based drug delivery systems. J Contr Release. 2001;73:137–72.
8. Lukyanov AN, Gao Z, Mazzola L, Torchilin VP. Polyethylene glycol-diacyllipid micelles demonstrate increased acculumation in subcutaneous tumors in mice. Pharm Res. 2002;19:1424–9.
9. Weissig V, Whiteman KR, Torchilin VP. Accumulation of protein-loaded long-circulating micelles and liposomes in subcutaneous Lewis lung carcinoma in mice. Pharm Res. 1998;15:1552–6.
10. Tang N, Du G, Wang N, Liu C, Hang H, Liang W. Improving penetration in tumors with nanoassemblies of phospholipids and doxorubicin. J Natl Cancer Inst. 2007;99:1004–15.
11. Wang Y, Wang R, Lu X, Lu W, Zhang C, Liang W. Pegylated phospholipids-based self-assembly with water-soluble drugs. Pharm Res. 2010;27:361–70.
12. Rijcken CJ, Snel CJ, Schiffelers RM, van Nostrum CF, Hennink WE. Hydrolysable core-crosslinked thermosensitive polymeric micelles: synthesis, characterisation and *in vivo* studies. Biomaterials. 2007;28:5581–93.
13. Yokoyama M, Fukushima S, Uehara R, Okamoto K, Kataoka K, Sakurai Y, Okano T. Characterization of physical entrapment and chemical conjugation of adriamycin in polymeric micelles and

their design for *in vivo* delivery to a solid tumor. J Contr Release. 1998;50:79–92.
14. Talelli M, Iman M, Varkouhi AK, Rijcken CJ, Schiffelers RM, Etrych T, *et al.* Core-crosslinked polymeric micelles with controlled release of covalently entrapped doxorubicin. Biomaterials. 2010;31:7797–804.
15. Hristova K, Needham D. Phase behavior of a lipid/polymer-lipid mixture in aqueous medium. Macromolecules. 1995;28:991–1002.
16. Ashok B, Arleth L, Hjelm RP, Rubinstein I, Onyüksel H. *In vitro* characterization of PEGlyated phospholipids micelles for improved drug solubilization: effects of PEG chain length and pc incorporation. J Pharm Sci. 2004;93:2476–87.
17. Arleth L, Ashok B, Onyuksel H, Thiyagarajan P, Jacob J, Hjelm RP. Detailed structure of hairy mixed micelles formed by phosphatidylcholine and PEGlyated phospholipids in aqueous media. Langmuir. 2005;21:3279–90.
18. Mayer LD, Bally MB, Loughrey H, Masin D, Cullis PR. Liposomal vincristine preparations which exhibit decreased drug toxicity and increased activity against murine L1210 and P388 tumors. Cancer Res. 1990;50:575–9.
19. Charrois GJ, Allen TM. Drug release rate influences the pharmacokinetics, biodistribution, therapeutic activity, and toxicity of pegylated liposomal doxorubicin formulations in murine breast cancer. Biochim Biophys Acta. 2004;1663:167–77.
20. Luecke RH, Ryan MP, Wosilait WD. A mathematical model and computer program for adriamycin distribution and elimination. Comput Meth Programs Biomed. 1985;20:23–31.
21. Hershman DL, McBride RB, Eisenberger A, Tsai WY, Grann VR, Jacobson JS. Doxorubicin, cardiac risk factors, and cardiac toxicity in elderly patients with diffuse B-cell non-Hodgkin's lymphoma. J Clin Oncol. 2008;26:3159–65.
22. van Hoesel QG, Steerenberg PA, Crommelin DJ, van Oort W, Klein S, Douze JM, *et al.* Reduced cardiotoxicity and nephrotoxicity with preservation of antitumor activity of doxorubicin entrapped in stable liposomes in the LOU/M Wsl rat. Cancer Res. 1984;44:3698–705.
23. Yagmurca M, Bas O, Mollaoglu H, Sahin O, Nacar A, Karaman O, Songur A. Protective effects of erdosteine on doxorubicin-induced hepatotoxicity in rats. Arch Med Res. 2007;38:380–5.
24. Injac R, Strukelj B. Recent advances in protection against doxorubicin-induced toxicity. Technol Cancer Res Treat. 2008;7:15–26.
25. Bertani T, Poggi A, Pozzoni R, Delaini F, Sacchi G, Thoua Y, *et al.* Adriamycin-induced nephrotic syndrome in rats: sequence of pathologic events. Lab Invest. 1982;46:16–23.
26. Weening JJ, Rennke HG. Glomerular permeability and polyanion in adriamycin nephrosis in the rat. Kidney Int. 1983;24:152–9.
27. Jaenke RS, Fajardo LF. Adriamycin-induced myocardioal lesions: report of a workshop. Am J Sur Pathol. 1977;1:55–60.
28. Philips FS, Giladoga A, Marrouardt H, Sternberg SS, Vidal PM. Some observations on the toxicity of adriamycin (NSC-123127). Cancer Chemother Rep. 1975;59:177–81.
29. van Hoesel QG, Steerenberg PA, Vos JG, Hillen FC, Dormans JA. Antitumor effect, cardiotoxicity, and nephrotoxicity of doxorubicin in the IgM solid immunocytoma-bearing LOU/M/WSL rat. J Natl Cancer Inst. 1984;72:1141–50.